

**Military Technical College
Kobry El-Kobbah,
Cairo, Egypt**



**7th International Conference
on Electrical Engineering
ICEENG 2010**

HVDC Systems Voltage Profiles Under Different Conditions for Interconnected power systems

By

Nagat Mohamed Kamel Abdel -Gawad

Faculty OF Engineering (Shoubra), Benha University

Abstract:

High voltage direct current (HVDC) electric power transmission systems are preferred, in some situations, to the common alternating current AC transmission systems as a means for bulk transmission of electrical power. Modern form of HVDC transmission uses, extensively, modern technology. Some AC electric power systems, which are required to be connected together, may not be synchronized. Therefore, they cannot be connected even if the distance between them is short. Also, in some circumstances, it is physically impossible, or highly impracticable, to connect them, even if they are synchronized. In such conditions, HVDC systems are considered to be the most effective method for connecting these systems.

Therefore, in this paper investigation of the performance of HVDC systems under different operating conditions are conducted. Models representing some actual HVDC systems, and giving voltage profiles produced under different conditions, and simulated using Matlab/Simulink. Corresponding computed results are obtained.

Keywords:

Transmission systems, HVDC system configurations, HVDC system performance.

1. Introduction:

Both of high-voltage direct current electric power transmission systems (HVDC) and alternating current transmission systems are used for transmission of electrical power. The technique of HVDC transmission first appeared in the 1930s in Sweden at ASEA. One of the first installations was used in the Soviet Union in 1951 between Moscow and Kashira, and another system was used in Gotland, Sweden in 1954 [1].

Conventional HVDC transmission system, compared with three-phase AC transmission systems, is superior in the following aspects [2]. HVDC transmission line cost and operating cost are less than those of its AC counterpart. It needs not operate synchronously between the two AC systems linked by HVDC. Finally, it is easy to control and adjust power flow, etc.

The main relevant components of a HVDC system, Figure 1, are as follows [3-6]:

- 1- The converter composed of thyristors or IGBTs which converts power from AC to DC.
- 2- The converter transformer, which transforms voltage level of the AC busbar to a suitable level.
- 3- The Smoothing reactor.
- 4- The Harmonic Filters (AC filter and DC filter).
- 5- DC Transmission cable.
- 6- Control system.

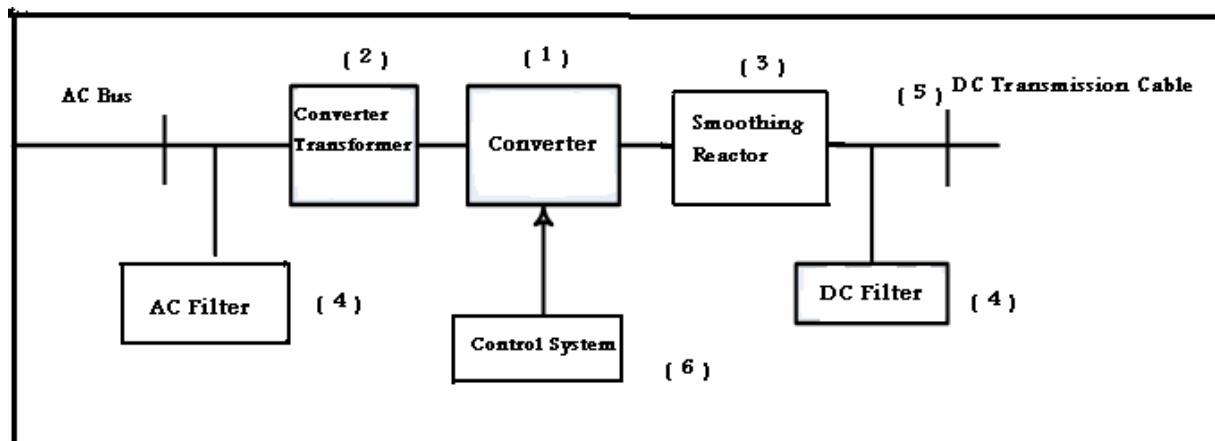


Figure (1): Main components of the HVDC system.

There are three types of high voltage DC links considered in HVDC applications which are monopolar, bipolar and homopolar links [7]. The monopolar link has one conductor, and uses either ground and/or sea returns. A metallic return can also be used where concerns for harmonic interference and /or corrosion exist. In applications with DC cables, a cable return is used. The bipolar link has two conductors, one is positive and the other is negative. Each terminal has two sets of converters connected in series and of equal ratings, on the DC side. The junction between the two sets of converters is grounded by the use of a short electrode line. Since both poles operate with equal

currents under normal operation, ground current flowing will be zero [7].

The third type is the homopolar, or multi terminal (MTDC), link, which has two conductors having the same polarity usually negative which, and can be operated with ground or metallic return.

Monopolar and bipolar links are the widely used type. The homopolar link has the advantage of reduced insulation costs, but it has the disadvantage of earth return that outweigh the advantages [8-10].

There are few studies that investigated the HVDC transmission systems under different operating conditions but not all possible operating conditions and profiles [11-16].

Therefore and taking into account the importance of power systems interconnections such that between Egypt and the neighboring countries, the main objective of this paper is to investigate in details the different profiles of the HVDC systems in different of working conditions, in order to assist in the design phases, determine the HVDC voltage levels developed over the line, determine suitable instrumentation and protection, and to, determine appropriate operation of converters used in the system. The obtained results are compared and agreed with great extent with pervious works [16]. All the models of the systems investigated in this paper have been simulated using Matlab/Simulink software package.

2. Method of Analysis and Case Studies:

Figure (2) presents a typical DC transmission system. To simulate the output DC power (P_D), voltage (V_D) and current (I_d) for such a system using a fully-controlled three-phase rectifier bridge, the following equations [7] are used at steady state, taking only the fundamental component of the current of the AC side of the converter. During the transition period, it is assumed that the demand load power is constant and equal to the average DC power.



Figure (2): Typical DC transmission system.

$$P_D = V_D \cdot I_D = \sqrt{3} \cdot V_{f-f} \cdot I_L \cos \phi . \quad (1)$$

$$I_P = I_L \cos \phi . , \quad I_Q = I_L \sin \phi . \quad (2)$$

$$I_P = \frac{a^2 \sqrt{3}}{4\pi\omega L_s} V_{f-f} [\cos 2\alpha - \cos 2(\alpha + \mu)] . \quad (3)$$

$$I_Q = \frac{a^2 \sqrt{3}}{4\pi\omega L_s} V_{f-f} [\sin 2(\alpha + \mu) - \sin 2\alpha - 2\mu] . \quad (4)$$

$$I_p = I_D \frac{a\sqrt{6}}{\pi} \left(\frac{\cos \alpha + \cos(\alpha + \mu)}{2} \right) . \quad (5)$$

$$V_D = \frac{P_D}{I_D} \quad (6)$$

Where,

=.....firing delay angle of thyristors.

V_M = ..the peak value of AC line-to-line voltage.

I_D =the output DC current.

I_L =the input AC line current.

a =turns ratio.

μ = ...overlap angle of the converter.

V_{f-f} = .. Input AC line-to-line voltage.

Two different models of the HVDC monopolar system and their control systems are considered and developed and investigated as follows.

2.1 Monopolar Model of a Transmission Line-Load System.

Figure (3) shows, 1000-MW-, 500-kV, 2-kA HVDC transmission system. This system is composed from a 500-kV, 5000-MVA AC network, a 3-phase 320 MVAR filter, 500/380 kV transformer, 6-pulse rectifier bridge, two smoothing reactors with 5 H each, 1000- MW, 500-kV, 2-kA, 300-km transmission line and a 242-kV DC load with an equivalent resistance of 5 Ω and equivalent inductance of 5 H. A shunt capacitor filter of 100 μ F can be connected on the DC side of the rectifier when it is required, to reduce the ripples of the output DC voltage waveforms of the rectifier. This system was simulated using Matlab/Simulink software package for the following cases.

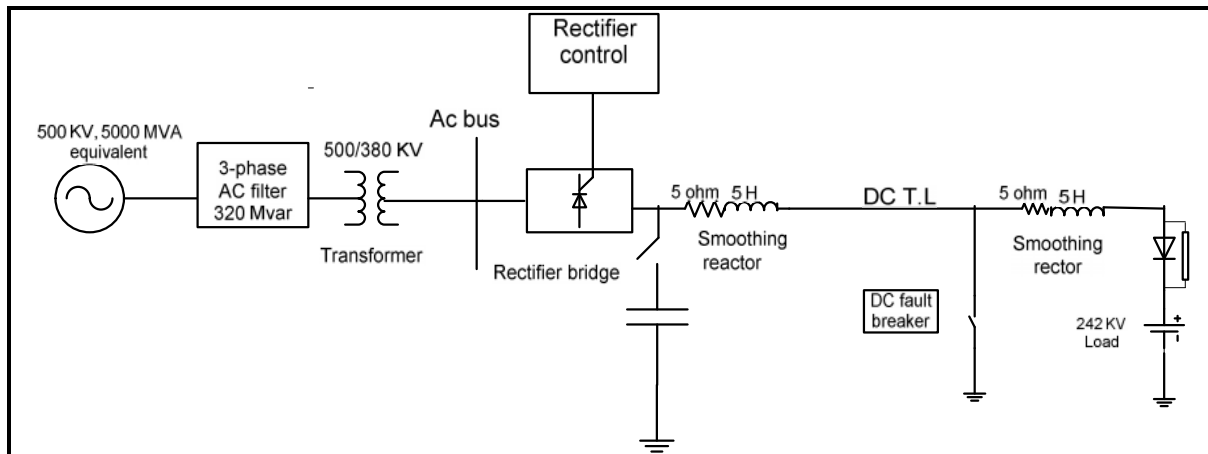


Figure (3): Simple line diagram representation of the HVDC monopolar system model.

2.1.1 System Profiles under Normal Operation Conditions

Figures (4) (a) and (4) (b) show the waveforms of the AC voltage and current input to the rectifier at normal condition when the system connected. It should be noticed that the value of the voltage over the simulated time is constant at the rated value of 1 pu. The AC current value increases, from zero pu to 1 pu, in 0.1 s. Figure (4) (c) shows the output DC voltage of the rectifier. It can be noticed that the DC voltage reached to steady state in 0.08 s and the output is almost, pure DC voltage, this is, because it is measured after compensator reactor of (R=5 ohm, L= 5 henry). Figure (4) (d) shows the output DC voltage with a shunt capacitor filter connected, without series smoothing reactor, this reduces the voltage waveforms ripples, compared with that shown in Figure (4) (c), with a series smoothing reactor.

Figures (5) (a, b) present the output DC current and input firing angle of the rectifier. The DC current start from zero and reaches a steady state in 0.05 s. Figure (5) (b) shows the firing angle (55 degrees) required to obtain 1 pu current. The obtained results, in this case show that, the parameters of the control system are properly identified.

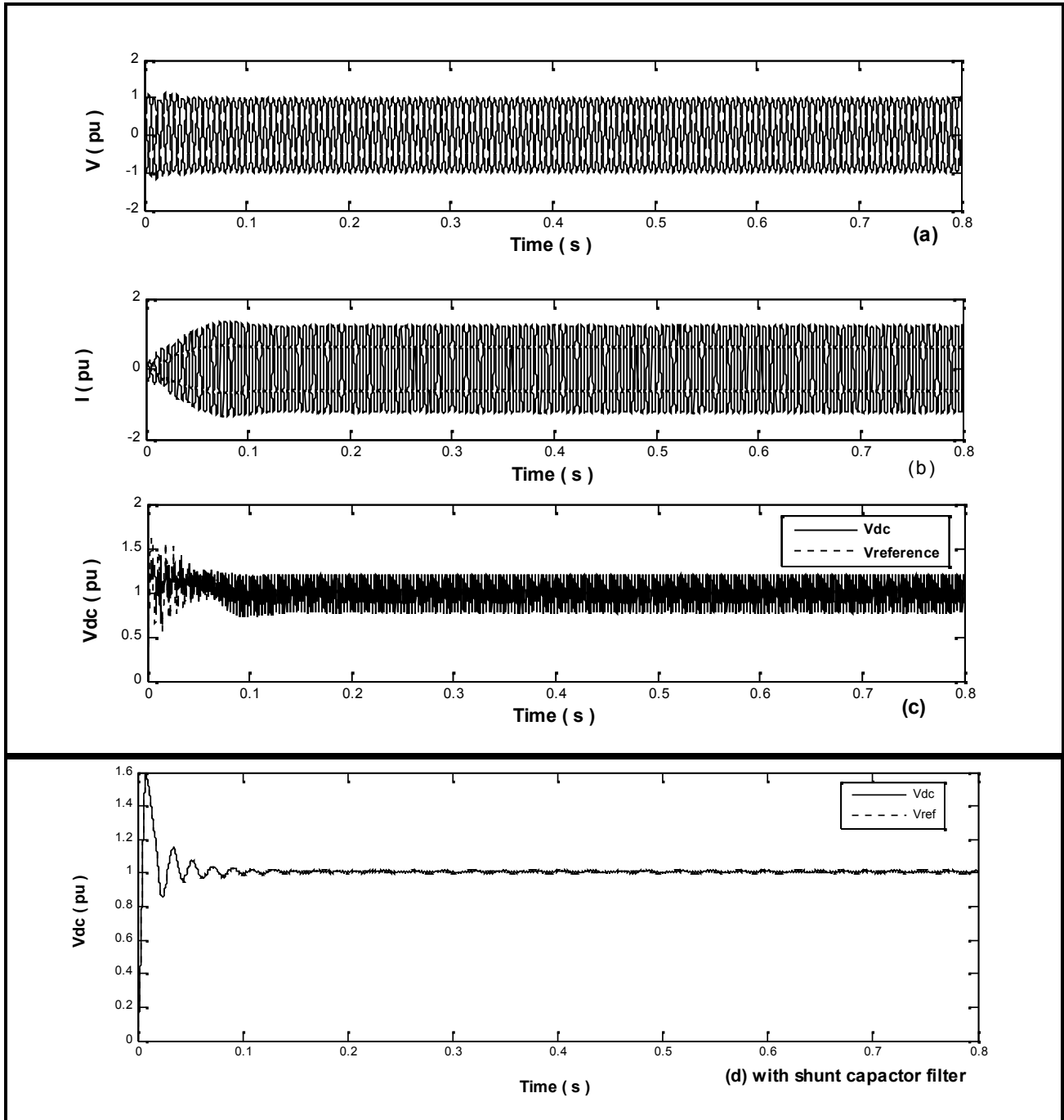


Figure (4): Input AC voltage, current and output DC voltage of the rectifier (in case of normal operation).

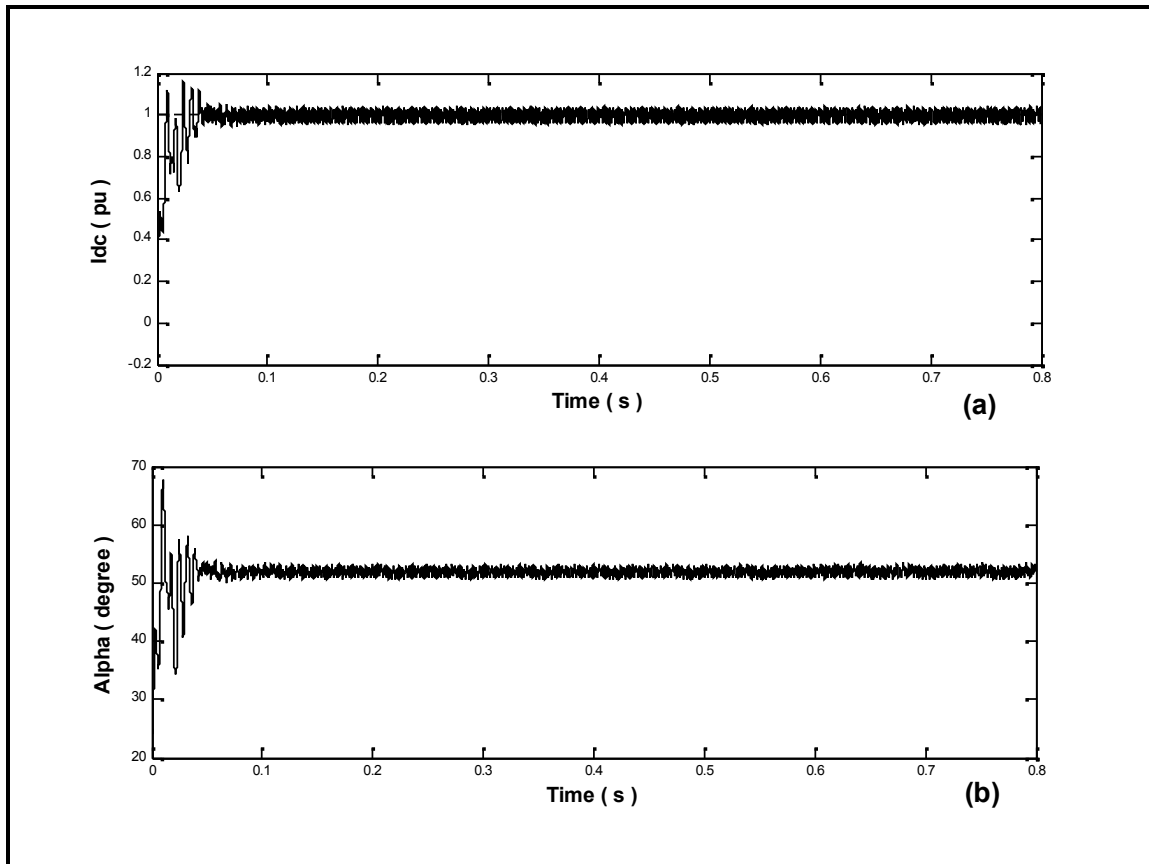


Figure (5): Output DC current and input firing angle of the rectifier (in case of normal operation).

2.1.2 System profiles under the condition of a Fault on the DC T.L.

Figures (6) (a, b) show the input AC voltage and current of the rectifier in case of, a fault condition, occurred at the DC T.L side. It can be noticed that, when a DC fault is applied, at time, $t = 0.5$ s, on the DC transmission line, the AC current increases to the value of 2 pu in 10 ms and the AC voltage decreased to zero and at $t = 0.55$ s the firing angle (alpha) is forced by the protection system and the rectifier is turned off. At $t = 0.555$ s the fault is cleared and at $t = 0.62$ s the AC voltage and current reach to steady state of 1pu. Also, as can be noticed in the figure (6) (d), the output DC voltage of the rectifier and it can be noted that, the DC voltage is the same as the case of normal operation condition, for the time period, from zero time to 0.5 s, of the considered time. When a DC fault is occurred on the line, from $0.5 < t < 0.55$ s, the DC voltage decreases to reach the zero value in 0.12 ms and at $t = 0.55$ s, the firing angle is forced by protection system to reach 165 degrees, the fault is cleared at $t = 0.555$ s. At $t = 0.57$ s, the regulator is released and starts to regulator the DC voltage again. The steady-state

1pu voltage is recovered and reached at $t= 0.65$ s. The results obtained in this case show that the parameters of the control/protections systems are properly identified.

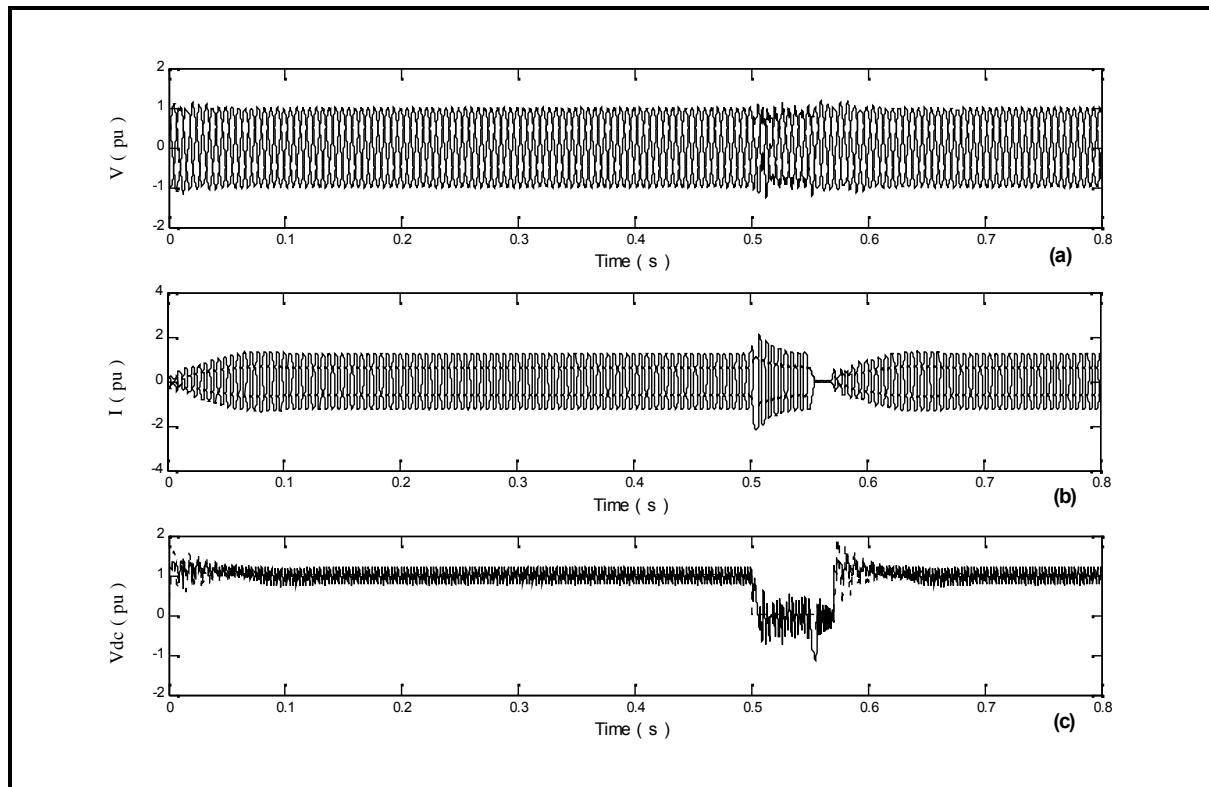


Figure (6): Input AC voltage, current and output DC voltage of the rectifier (in case of DC fault on DC T.L).

Figures (7) (a, b, c) represent the output DC current, input firing angle of the rectifier and the DC fault current. It can be noticed that the value of the output DC current and firing angle of the rectifier for the time period, from $0 < t < 0.5$ s, is nearly, the same as, in the case of normal operation condition. When in the time period, $0.5 < t < 0.55$ s, a DC fault is applied on the DC line, starting at $t = 0.5$ s. The fault current increases to the value of 5 kA and the (DC) current increase to the value of 2 Pu (4 kA) in 10 ms. The fast regulator action lowers the current back to its reference value of zero Pu. For $(0.55 < t < 0.57$ s) at $t = 0.55$ s, the firing angle, input to the current regulator, is forced by the protection system to reach 165 degrees. The rectifier passes in inverter mode and send the energy stored in the line back to the 500 kV network. As a result, the arc current producing the fault rapidly decreases. The fault is cleared at $t = 0.55$ s, when the current zero crossing is reached. From $(0.57 < t < 0.8$ s) at $t = 0.57$ s, the regulator is released and it starts to regulate the DC current again. The steady-state is reached and

the system is recovered at $t=0.65$ s. The results obtained in this case show that the parameters of the control/protections systems are properly identified.

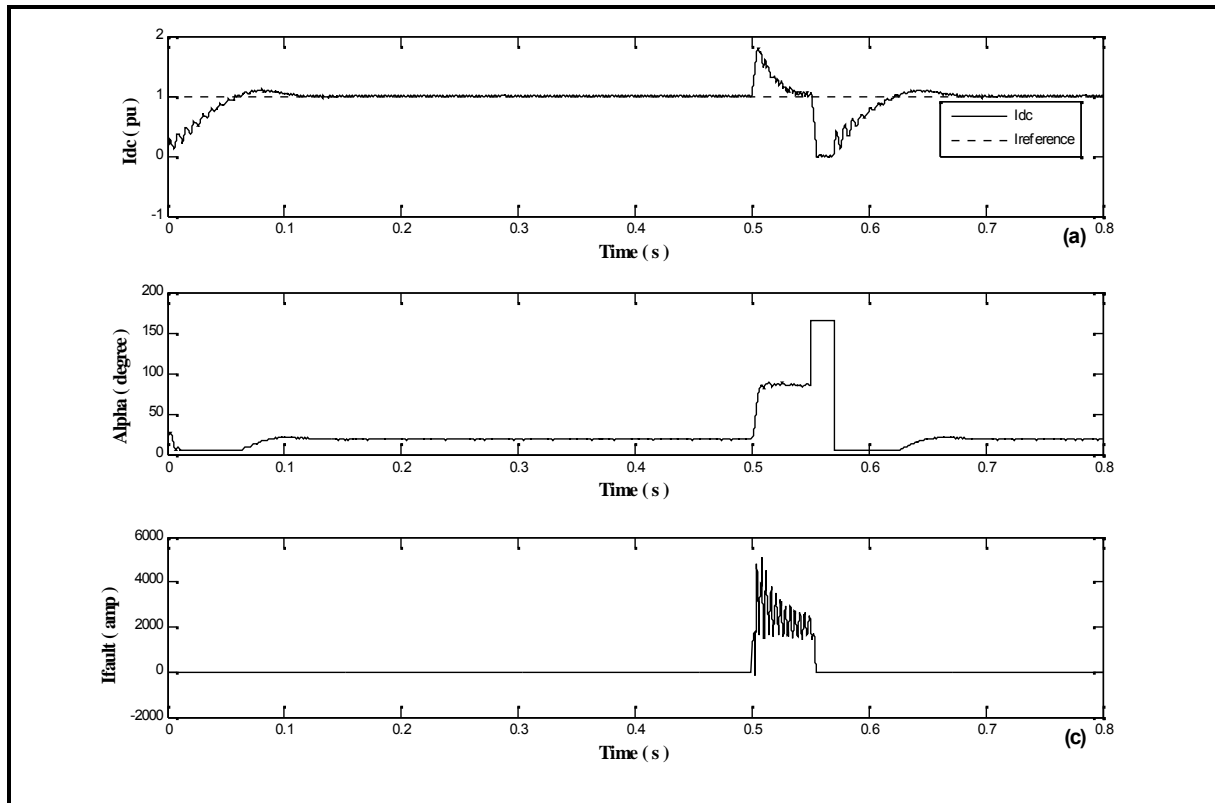


Figure (7): Output DC current and input firing angle of the rectifier (in case of a DC fault on DC T.L).

2.1.3 Effect of Transmission Line Length:

Figures (8) (a, b) and Figure (4) (d) show the output DC voltages of the rectifier, in case of long transmission line (500 Km) and short line (80 km) and medium line (300 km), with shunt capacitor filter is connected in the DC side, respectively. It can be noted that, the longer the transmission line length is, the lower is the voltage waveforms distortion and ripples on the HVDC systems.

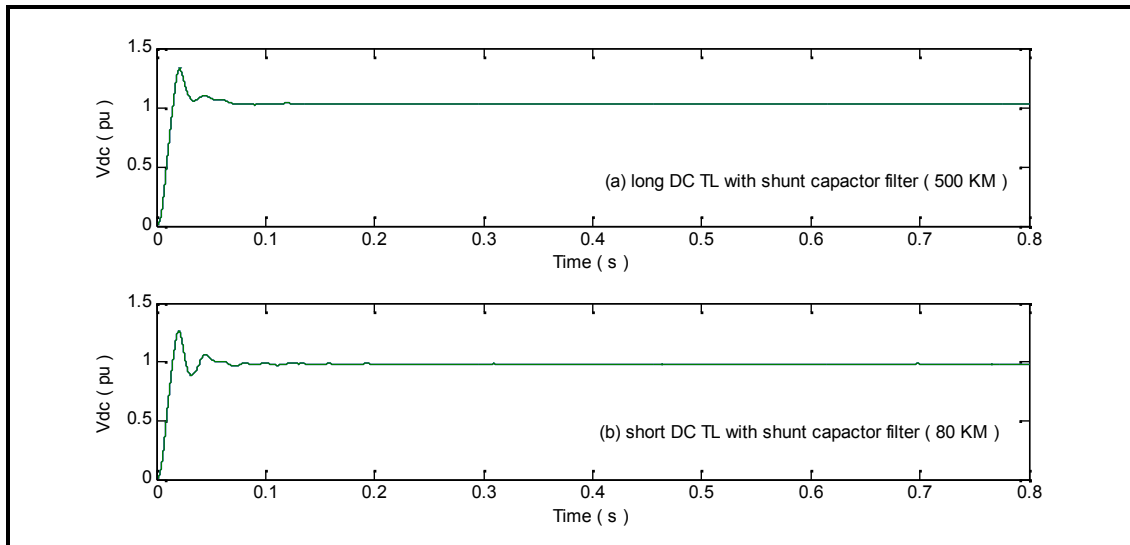


Figure (8): Output DC voltage of the rectifier in case of long and short TL (with shunt capacitor filter).

2.2 Monopolar model of Two High Voltage Substations Connection System.

Figure (9) shows the second developed model which consists mainly from a 1000-MW (500-kV, 2-kA), DC interconnection which is used to transmit power from a (500-kV, 5000-MVA, 60-Hz) network to a (345-kV, 10,000-MVA, 50-Hz) network. The rectifier and the inverter are 12-pulse converters using two 6-pulse thyristor bridges connected in series. The rectifier and the inverter are interconnected through a 300-km distributed DC line and two smoothing reactors (5 , 5 H), each.

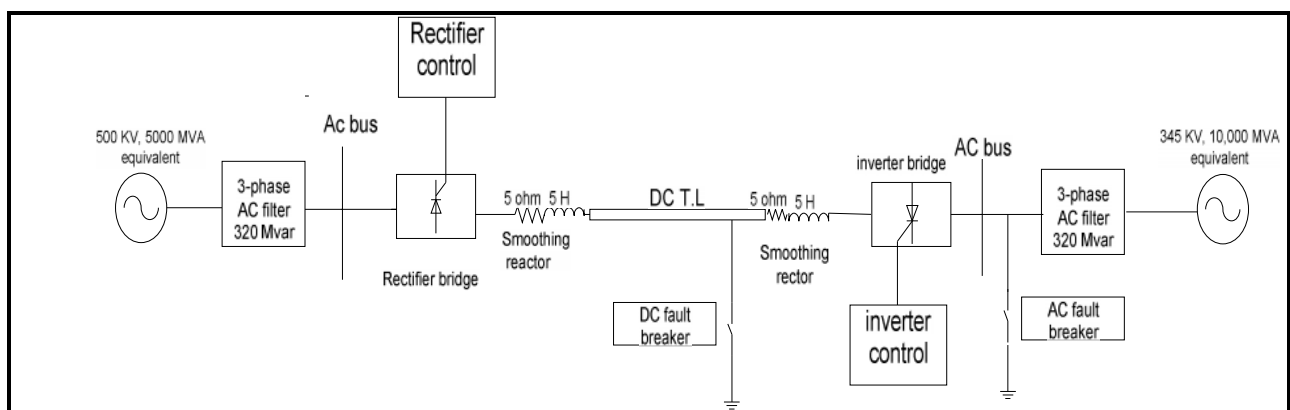


Figure (9): HVDC 12-pulse Transmission System, 1000 MW (500kV-2kA), 50/60 Hz.

2.2.1 System Profiles under Normal Operation Condition

Figures (10) (a, b, c) show the output DC voltage, current and firing angle of the rectifier in case of the system normal operation condition. At the end of this first ramp ($t= 0.32$ s) the DC line is charged at its nominal voltage and the DC voltage reaches steady state. At the time, $t = 0.4$ s, the current is ramped from 0.0 pu to 1 pu (2KA) in 0.18 s (5 pu /s). At the time instant of ($t =0.58$ s), the DC current reaches steady state. The current is controlled by the rectifier while the voltage is controlled by the inverter. It can be noticed that the current stabilizes in approximately 0.1 sec. Figure (10) (c) of the figure shows the firing angle, and it can be noted that in the steady-state, the firing angle (alpha) is 16.5 degrees. At $t =1.4$ s the stop sequence is initiated by ramping down the current to 0.1pu. At $t =1.6$ s, a forced-alpha of the rectifier extinguishes the current. At $t= 1.7$ sec, the pulses are blocked in the rectifier. The results obtained in this case show that the parameters of the control system are properly identified.

Study is carried out for the effect of variable transmitted (transferred) power between the two interconnected systems. It is noticed that the variable power would not varied the voltage profile but the amplitude is only affected.

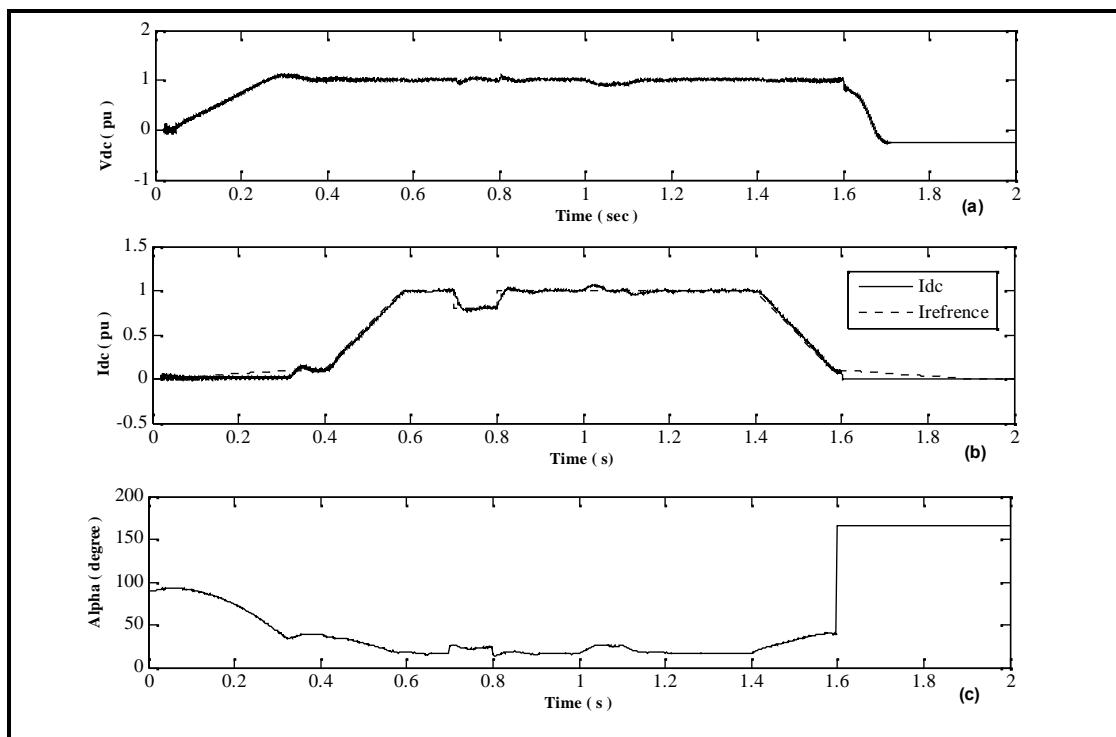


Figure (10): The output DC voltage, and DC current and firing angle of the rectifier (in case of (Normal operation)).

2.2.2 Effect of a Fault on DC Transmission Line.

Figures (11) (a, b) show the AC voltage and current input to the rectifier in case of a DC fault occurred on the DC transmission line. It can be noticed that the value of current, in the time period, from (0 s to 0.4 s), equal zero (starting interval), while the AC voltage equal 1 Pu over the considered time. After a time of 0.4 s, the AC current reaches to 1pu. When a DC fault is applied, at the time $t = 0.7$ s, on the DC transmission line the AC current increase to 2.3 pu and the AC voltage reaches to zero. The fault is continuous to the time of $t = 0.77$ s, then the protection operation starts by increasing firing angle of the rectifier to 165 degrees. The firing angle (alpha) is released at $t = 0.87$ s and the AC voltage and current recover in 0.4 s. At $t = 1.4$ s the stop sequence is initiated by ramping down the current to 0.1pu. At $t = 1.6$ s a forced-alpha at the rectifier extinguishes the current. At $t = 1.7$ s, the pulses are blocked in the rectifier.

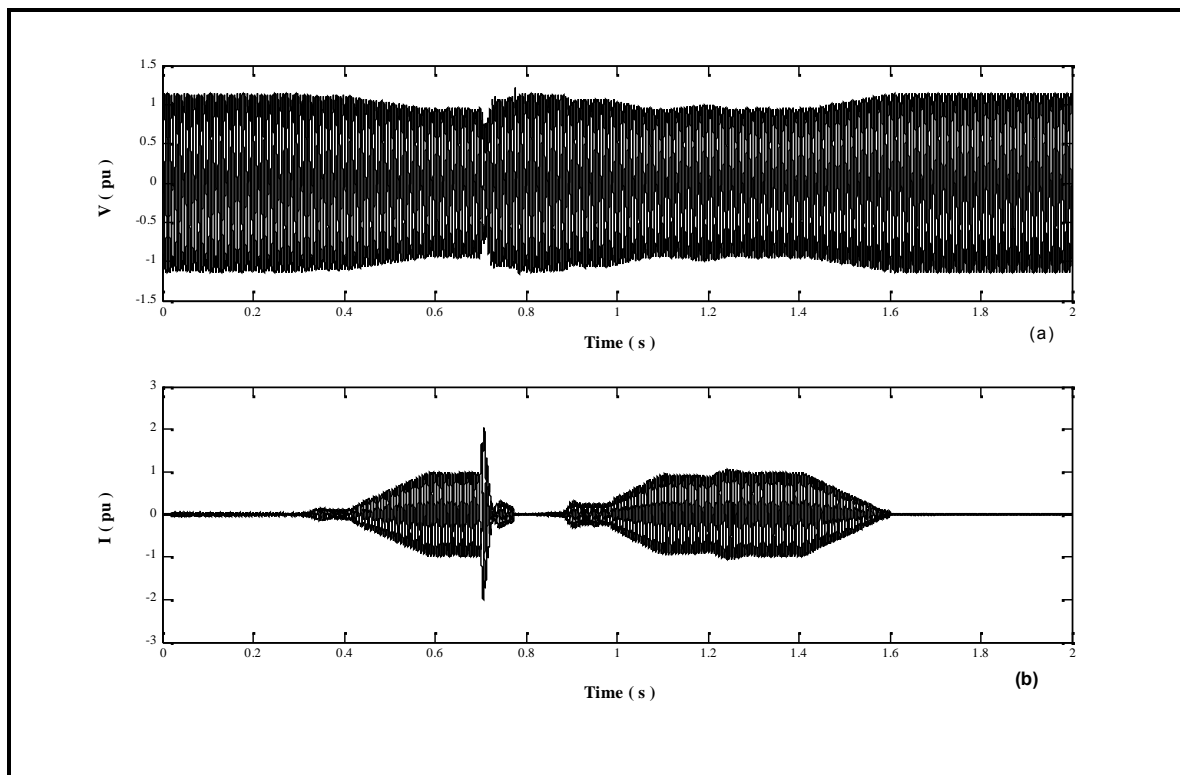


Figure (11): Input AC voltage and current to the rectifier (in case of a DC fault on DC T.L).

Figures (12) (a, b, c) show the output DC voltage, current and input firing angle of the rectifier in case of a DC fault occurred on the DC transmission line. At starting the

output DC voltage and current equal zero, then the DC voltage increases to its nominal value (1 pu) at $t = 0.32$ s, while the current increases to the value of 1 pu at $t = 0.58$ s. Under the fault condition, at $t = 0.7$ s, the DC current quickly increases to 2.3 pu and the DC voltage falls to zero at the rectifier. The DC current is still continuous to circulate in the fault. Then, at $t = 0.77$ s, the rectifier firing angle is forced to the value of 166 degrees by the DC protection system because a DC voltage drop is detected ($V_d < 0.5$ Pu for 70 ms). The rectifier operates in interval mode. The DC line voltage becomes negative and the energy stored in the line is returned to the AC network, causing rapid extinction of fault current at next zero-crossing. Then, the firing angle (alpha) is released at $t = 0.87$ s and the normal DC voltage and current recover in approximately time of 0.4 s. In Figure (12) (c), it can be noticed that the firing angle, during the fault condition, increased to 165 degree to turn off the rectifier bridge. The results obtained in this case show that the parameters of the control/protections systems are properly identified.

Study is carried out for the effect of variable transmitted (transferred) power between the two interconnected systems, while a fault is occurred on the DC line. It is noticed that the variable power would not vary the voltage profile but the amplitude is only affected.

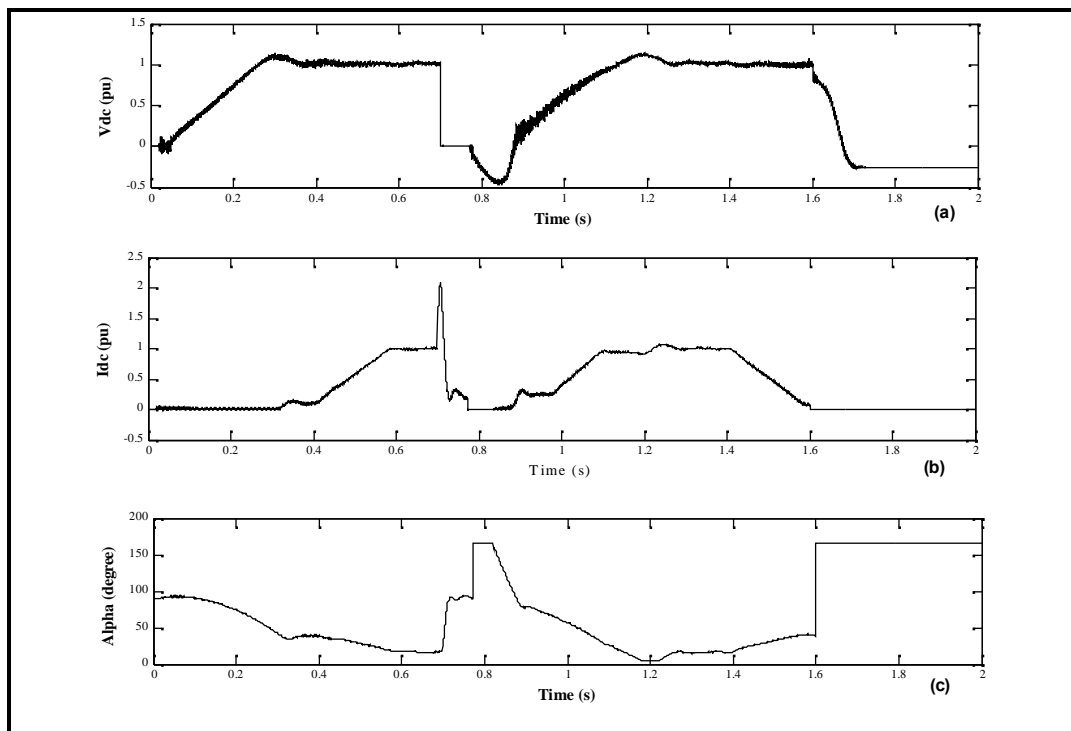


Figure (12): The output DC voltage, DC current and firing angle of the rectifier (in case of DC fault on a DC T.).

3. Conclusions:

Different model systems of HVDC transmission systems are simulated and investigated under a variety of loading operation conditions. The simulation models and control system are built and developed based on Matlab/Simulink package. Through this study the different obtained HVDC systems voltage profiles are investigated and analyzed to be used as a help toll in the design phase of the HVDC systems. Some main points have been concluded:

- 1- The HVDC voltage profile of the DC side could be controlled and stabilized through controlling the feedback signal of the DC load current.
- 2- The longer is the DC line; the lower is the DC voltage/current distortion.
- 3- The fault DC current can reach about 2 pu under the fault at the DC line conditions.
- 4- The fault occurred on the DC side affects the AC side of both the rectifier and the inverter with wave distortion.
- 5- The AC fault in both sides of the inverter and the rectifier has the same affects as, the case of, the fault at DC lines.
- 6- Varying the transmitted (transferred) power between the two interconnected systems would not vary the voltage profile but the amplitude is only affected.

References:

- [1] Alessandro Clerici, Luigi Paris, Per Danfors, "HVDC conversion of HVAC lines to provide substantial power upgrading", IEEE Transactions on Power Delivery, Vol. 6, No.1, January 1991.
- [2] Szuki Hirokazu, Ajima Tatsugito, "Development and testing of prototype models for a high-performance 300 MW self-commuted AC/DC converter", IEEE Transactions on Power Delivery, vol. 12, pp. 1589-1597, April 1997.
- [3] Dennis A. Woodford, "HVDC Transmission", Manitoba HVDC Research Centre, 400-1619 Pembina Highway, Winnipeg, Manitoba, R3T3Y6, Canada, 18 Marsh 1998.
- [4] J. Bradley III, et al, "OPERATIONAL EXPERIENCE WITH TWO TYPES OF 2 MW HVDC POWER SUPPLIES ON LEDA", Proceedings of the 1999 Particle Accelerator Conference, New York, 1999.

- [5] Sastry Kumganty, "HVDC Transmission System Models For Power System Reliability Evaluation", IEEE cat.No.95/CH3581-6/0-7803- x/95/s3@1995IEEE, 1995.
- [6] T. Hasegawa, K.Yamaji and H. Imkawa, "Development of a Thyristor Valve for Next Generation 500kV HVDC Transmission Systems", IEEE Transactions on Power Delivery, Vol. 1 I, No. 4, October 1996.
- [7] MUHAMMAD H. RASHID,"POWER ELECTRONICS HANDBOOK", Library of Congress Catalog Card Number: 00-2001088199, International Standard Book Number: 0-12-581650-2, ACADMIC PREES, A Harcourt Science and Technology Company, New York / Canada, 2001.
- [8] D. M. Larruskain, et al, "Transmission and Distribution Networks: AC versus DC", www.ehu.es.
- [9] K. R. Padiyar and Nagesh Prabhu, "Modelling, Control design and Analysis of VSC based HVDC Transmission Systems", Power System Technology - POWERCON 2004 Singapore, 21-24 November 2004.
- [10] D. Sudarmadi, G. C. Paap2 and L. v.d. Sluis, "Planning Issues for Java-Sumatera HVDC Interconnection"., Proceedings of the International Conference on Electrical Engineering and Informatics Institute Technology Bandung, Indonesia, June 17-19, 2007.
- [11] Tanaka, Toshihiko, Nakazato and et al, " A new approach to the capacitor-commutated converter for HVDC - A combined commutation-capacitor of active and passive capacitors", Proceedings of the IEEE Power Engineering Society Transmission and Distribution Conference, v 2, n WINTER MEETING, 2001, p 968-973, IEEE Power Engineering Society Winter Meeting, Jan 28-Feb 1, 2001.
- [12] Asplund, G.BB Power Syst. AB, Ludvika, "Application of HVDC Light to power system enhancement", Power Engineering Society Winter Meeting, IEEE, v 14, p 2498-2503, Jan 2000.
- [13] Chamia, M., "HVDC – A major option for the electricity networks of the 21st Century", IEEE WPM 1999 – Panel Session, The Role of HVDC Transmission in the 21st Century, November 2001.
- [14] Vancers, I., Christofersen, D.J., Leirbukt, A., Bennett, M.G., "A Survey of the reliability of HVDC Systems Throughout the World During 1999-2000.", CIGREE Paper No.14-101, 2002.
- [15] K. R. Padiyar and Nagesh Prabbhu, "Modelling, Control design and Analysis of VSC based HVDC Transmission Systems", 2004 International Conference on Power System Technology- POWERCON 2004, Singapore, PP. 774-774, 21-24 November 2004.
- [16] Chengyong Zhao, Haibo Cui and Gengyyin Li, "A Novel HVDC Transmission System with Parallel Large Capacitor Connected in the DC Side of the Rectifier and Its Technical Feasibility", 2005 IEEE/PES Transmission and Distribution Conference & Exhibition: Asia and Pacific, Dalian, China, 2005.